J Mater Sci: Mater Med (2013) 24:2145–2155
DOI 10.1007/s10856-013-4971-9

Biological evaluation of alginate-based hydrogels, with antimicrobial features by Ce(III) incorporation, as vehicles for a bone substitute

D. S. Morais · M. A. Rodrigues · M. A. Lopes · M. J. Coelho · A. C. Maurício · R. Gomes · I. Amorim · M. P. Ferraz · J. D. Santos · C. M. Botelho

Received: 31 January 2013 / Accepted: 31 May 2013 / Published online: 12 June 2013

Abstract A novel hydrogel, based on an alginate/hyaluronate mixture and Ce(III) ions, with effective bioactive and antimicrobial ability was developed to be used as vehicle of a synthetic bone substitute producing an injectable substitute (*IBS*). Firstly, three different *IBS*s were prepared using three developed alginate-based hydrogels, the hydrogel *Alg* composed by alginate, the hydrogel *Alg/Ch* composed by an alginate/chitosan mixture and the hydrogel *Alg/HA* composed by an alginate/hyaluronate mixture. MG63 cells viability on the *IBS*s was evaluated, being observed a significantly higher cell viability on the *Alg/HA_IBS* at all time points, which indicates a better cell adaptation to the material, increasing their predisposition to produce extracellular matrix and thus allowing a better bone regeneration. Moreover, SEM analysis showed evident filopodia and a spreader shape of MG63 cells when seeded on *Alg/HA_IBS*. This way, based upon the in vitro results, the hydrogel *Alg/HA* was chosen to the in vivo study by subcutaneous implantation in an animal model, promoting a slight irritating tissue response and visible tissue repairing. The next step was to grant antimicrobial properties to the hydrogel that showed the best biological behavior by incorporation of Ce(III) ions into the *Alg/HA,* producing the hydrogel *Alg/HA2*. The antimicrobial activity of these hyaluronate-based hydrogels was evaluated against *Staphylococcus aureus*, *Staphylococcus epidermidis, Pseudomonas aeruginosa* and *Candida albicans*. Results showed that Ce(III) ions can significantly enhance the hydrogel antimicrobial ability without compromising the osteoconductivity improvement promoted by the vehicle association to the synthetic bone substitute.

1 Introduction

Bone defects regeneration remains a concern due to their high incidence in people of different ages, limiting their life quality. In the last few decades, synthetic bone substitutes have been developed in an attempt to solve this medical challenge of bone regeneration [1, 2]. For instance, glass-reinforced hydroxyapatite (GR-HA) composites are

D. S. Morais and M. A. Rodrigues have contributed equally to this study.

D. S. Morais · C. M. Botelho
Instituto de Biotecnologia e Bioengenharia, Centro de Engenharia Biológica, Universidade do Minho, Campus de Gualtar, 4710-057 Braga, Portugal

M. A. Rodrigues · M. A. Lopes (✉) · J. D. Santos
CEMUC, Departamento de Engenharia Metalúrgica e Materiais, Faculdade de Engenharia, Universidade do Porto, Rua Dr. Roberto Frias, 4200-465 Porto, Portugal
e-mail: malopes@fe.up.pt

M. J. Coelho · M. P. Ferraz
CEBIMED—Centro de Estudos em Biomedicina, Faculdade de Ciências da Saúde, Universidade Fernando Pessoa (FCS-UFP), Porto, Portugal

A. C. Maurício · R. Gomes
Centro de Estudos de Ciência Animal (CECA), Instituto de Ciências Agrárias e Agro-Alimentares (ICETA), Universidade do Porto, Porto, Portugal

A. C. Maurício · R. Gomes · I. Amorim
Instituto de Ciências Biomédicas Abel Salazar (ICBAS), Universidade do Porto (UP), Rua de Jorge Viterbo Ferreira, 4050-313 Porto, Portugal

I. Amorim
Instituto de Patologia Molecular e Imunologia da Universidade do Porto (IPATIMUP), Rua Dr. Roberto Frias, 4200-465 Porto, Portugal

calcium phosphate-based substitutes able to chemically mimic the bone inorganic phase. Their osteoconductive behavior seems to create an ideal environment for bone cells adhesion and proliferation, promoting bone regeneration [3–5].

Synthetic bone substitutes have been associated with hydrogels in order to turn the substitutes injectable, what is advantageous in some clinical applications that present difficulties in the access to the bone defect, namely in the augmentation of osteoporotic fractures, in some applications in the spine and in the treatment of maxillofacial defects. Besides, this minimally invasive surgical approach can decrease the surgery time and provides a faster and more economic recovery of the patient [6, 7]. Moreover, the hydrogel association can improve the osteoconductive properties of the synthetic bone substitutes and even grant them osteoinductive and osteogenic properties by the incorporation of growth factors and stem cells within the gel [8–12].

Natural polysaccharides are very promising molecules for tissue engineering applications, since they present high biocompatibility and resemble glycosaminoglycans of the extracellular matrix (ECM). These polymers have shown a lower stimulation of immunological reactions than some synthetic polymers [13, 14]. Alginate is a natural biodegradable linear block co-polymer composed of two monomers, β-D-mannuronic acid and α-L-guluronic acid, which are linked by (1–4) glycosidic bonds. This natural polysaccharide has been used to produce hydrogels by the simple addition of divalent cations, such as Ca^{2+}, which bind to monomers carboxylic groups providing the cross-linking of the polymeric chains and thus the gelation of the alginate solution [15–17]. However, alginate has the biomedical disadvantage of presenting a lower cell adhesion than other natural polymers by promoting a very low protein adsorption and cell attachment due to its negative charge and high hydrophilicity [18–20]. Thus, in order to improve the cell adhesion on alginate, this polymer can be easily associated with another polyelectrolyte that allows a better cell adhesion.

Chitosan is a natural biodegradable polycation composed by the monomers D-glucosamine and *N*-acetyl-D-glucosamine linked by β(1–4)-glycosidic bond and it has been used in biomedical applications as a promoter of cell adhesion, proliferation and differentiation [13, 21, 22]. Hyaluronic acid is a natural biodegradable polyanion composed by monomers D-glucuronic acid and *N*-acetyl-D-glucosamine, linked by β(1–3) and β(1–4) glycosidic bonds [23, 24]. This polymer is the main component of ECM, being found in connective tissues and it is involved in different biological processes, namely, in morphogenesis, wound repair, inflammation and metastasis, through the interaction with cellular receptors [23, 25]. Hyaluronic acid has also a strong potential in bone repair, since it is found in high concentrations in the fracture callus, inhibiting the osteoclasts differentiation and even participating in the migration of mesenchymal stem cells [26–28].

In every surgical procedure there is the major risk of infection that presents serious consequences, which can compromise the recovery success. To prevent those infections, several approaches have been tried, such as sterility protocols and antibiotics administration. However, these protocols are not always effective and the antibiotic activity can even fail due to pathogenic resistance development [29, 30]. Therefore, recently, studies were made to ascertain the use of certain ions as antimicrobial agents, such as cerium (Ce), which has revealed antimicrobial properties against several microorganisms. This way, it can be incorporated in different biomaterials to grant them antimicrobial ability, contributing to a better implant performance [31–33].

The purpose of this study was to evaluate the biological performance in vitro and in vivo of three hydrogels previously developed based on alginate, chitosan and hyaluronic acid, which should enhance the osteoconductive properties of the bone substitute (GR-HA). Furthermore, in order to obtain a hydrogel not only with an osteoconductive ability but also with an antimicrobial ability to avoid infections, Ce(III) ions were incorporated in one of these hydrogels and its biological performance was also studied.

2 Materials and methods

2.1 Materials

Alginic acid sodium salt from brown algae (bioreagent grade; low viscosity; 39 % of guluronic acid and 61 % of mannuronic acid), hyaluronic acid sodium salt from *Streptococcus equi,* calcium chloride hexahydrate ($CaCl_2 \cdot 2H_2O$, medical grade) and cerium(III) nitrate hexahydrate ($Ce(NO_3)_3 \cdot 6H_2O$) were purchased from *Sigma* (USA). Chitosan HCl (medical grade) was purchased from *Heppe Medical Chitosan GmbH* (Germany) and the hydroxyapatite (HAP) powder was purchased from *Plasma Biotal* (UK).

2.2 Methods

2.2.1 Hydrogels preparation

Three hydrogels were prepared according to the already optimized protocol described in our previous work [34]. Briefly, an alginate hydrogel (*Alg*) was prepared by adding a $CaCl_2$ solution (15×10^3 mg/L) to a sodium alginate solution (7 % (w/V)) in a proportion of 1:4 (V_{CaCl2}:V_{sodium}

$_{alginate}$). An alginate/chitosan based hydrogel (*Alg/Ch*) was prepared by adding a chitosan HCl solution (0.5 % (w/V)) to the $CaCl_2$ solution, and then the alginate solution, according to the proportions: 1:4 (V_{CaCl2}:$V_{sodium\ alginate}$) and 1:1 ($V_{chitosan\ HCl}$:$V_{sodium\ alginate}$). An alginate/hyaluronate based hydrogel (*Alg/HA*) was prepared by adding a sodium hyaluronate solution (0.5 % (w/V)) to the alginate solution followed by the addition of the $CaCl_2$ solution in the proportions: 1:1 ($V_{sodium\ hyaluronate}$:$V_{sodium\ alginate}$) and 1:4 (V_{CaCl2}:$V_{sodium\ alginate}$).

In addition, two other alginate/hyaluronate based hydrogels with Ce(III) were prepared using cross-linking solutions with different Ce(III) concentrations. One solution was prepared using 15×10^3 mg/L of $CaCl_2$ and 6.6×10^2 mg/L of $Ce(NO_3)_3$ and other also using 15×10^3 mg/L of $CaCl_2$, but with 13.2×10^2 mg/L of $Ce(NO_3)_3$. Then, each solution was added, in a proportion of 1:4 ($V_{cross\text{-}linking\ solution}$:$V_{sodium\ alginate}$), to the alginate/hyaluronate mixture obtaining the hydrogel *Alg/HA1* and *Alg/HA2,* respectively.

2.2.2 Glass reinforced hydroxyapatite (GR-HA) and injectable bone substitutes (IBSs) preparation

GR-HA was obtained by adding 2.5 % (w/w) of glass (with the composition $65P_2O_5$–$15CaO$–$10CaF_2$–$10Na_2O$, mol%) to HAP mixed with microcrystalline cellulose. Then, discs were prepared by uniaxial pressing and heat treated at 600 °C to burn out the microcrystalline cellulose and then sintered at 1,300 °C for 1 h. Finally the discs were milled and sieved to produce granules of a 500–1,000 μm size range.

Five different *IBS*s were prepared by just mixing and aggregating the GR-HA granules with each one of the developed hydrogels, in the proportions that have already been optimized in our previous work [34].

It should be noted that before the hydrogels preparation the raw materials were appropriately sterilized. The sodium alginate powder was sterilized in an autoclave (121 °C for 15 min), after proving by FTIR–ATR (Fourier transform infrared–attenuated total reflectance) spectroscopy analysis that this method does not alter the polymer chemical structure, and its solution was prepared under sterile conditions. All the other polymeric solutions were filtered also under sterile conditions and GR-HA granules were sterilized in an autoclave (121 °C for 15 min).

2.2.3 Cell viability evaluation

2.2.3.1 Cell culture MG63 human osteosarcoma cells were seeded in 75 cm^2 flasks with 10 mL of α-MEM (α-minimal essential medium, *Gibco*, USA), supplemented with 10 % (V/V) of fetal bovine serum and 1 % (V/V) antibiotic–antimycotic solution (*PAA,* Germany), in a humidified atmosphere, with 5 % CO_2, at 37 °C. The culture medium was changed every 2 days.

2.2.3.2 MTT assay Firstly, 0.6 mL samples of each *IBS* were placed on 24-well plates. Then, 1 mL of MG63 cell suspension (2×10^4 cells/mL) was seeded on the surface of each sample and the plates were incubated, at 37 °C, in a 5 % CO_2 humidified atmosphere, for different time periods (24, 48 and 72 h). As comparative model, for the same time points, wells with cells seeded on GR-HA granules were used. Ethanol (96 % (V/V)) was added to wells with cell suspension as null cell viability control, while simple cell suspension was used as cell viability control.

After each incubation period, the cells viability was measured using the MTT assay (3-[4,5-dimethyl-thiazol-2-yl]-2,5-diphenyltetrazolium bromide, *Sigma*, USA) according to the manufacture instructions. The absorbance was measured at 565 nm (with a 630 nm background) using the microplate reader *STAT FAX 3200* (*Awareness Technology*, USA). This experiment was performed in triplicate for each *IBS* and GR-HA granules.

2.2.4 Scanning electron microscopy (SEM) analysis

The morphology of the osteoblastic human cells seeded on the surface of *Alg_IBS*, *Alg/Ch_IBS* and *Alg/HA_IBS*, after a contact period of 24 h, was analyzed by SEM. Briefly, samples with cells were firstly fixed with 1.5 % (m/V) glutaraldehyde in 0.14 M sodium cacodylate buffer (pH 7.4). Afterwards, samples were dehydrated using graded ethanol solutions from 50 % (V/V) to 100 % (V/V), followed by immersion in hexamethyldisilazanes (HMDS) solutions ranging from 50 % (V/V) to 100 % (V/V). The samples lasted 10 min in each ethanol and HMDS solution and overnight in 100 % (V/V) HMDS. All used reagents were purchased from *Sigma* (USA).

Finally, samples were placed onto aluminum stubs and coated with gold/palladium using a sputter coater (*SPI*, USA) for SEM analysis in a *Quanta 400FEG SEM* microscope (*FEI*, USA).

2.2.5 Subcutaneous implantation in Sprague–Dawley® rats

All surgical procedures were performed with the approval of the Veterinary Authorities of Portugal in accordance with the European Communities Council Directive of November 1986 (86/609/EEC). The hydrogel *Alg/HA* was implanted in three adult male Sprague–Dawley® rats (*Charles River*, Spain) that were fed with standard chow and water ad libitum. Adequate measures were taken to minimize pain and discomfort taking into account human

endpoints for animal suffering and distress. Animals were housed for 2 weeks before entering the experiment. For surgery, rats were placed in prone position under sterile conditions and the skin from the clipped dorsal area scrubbed in a routine fashion with antiseptic solution. Anaesthesia was achieved with an intra-peritoneal injection of a pre-mixed solution consisting in ketamine (*Imalgène 1000*®), 100 mg/kg body weight (bw), and xylazyne (*Rompun*®), 200 mg/kg bw.

Four 1.5–2 cm long linear incisions were made on the dorsal area. After dissection towards the ventral aspect of the body, 1 mL of the tested hydrogel was subcutaneously injected in one incision, one was left unfilled and served as control (the skin and subcutaneous tissues were collected on the surgery day), and the other two served as sham controls (the incisions were performed and empty closed). Skin and subcutaneous tissues were closed with a simple-interrupted suture of a non-absorbable filament (*Synthofil*®). An antibiotic (enrofloxacin, *Alsir*® 2.5 %, 5 mg/kg bw, subcutaneously) was administered to prevent any infections. 2 weeks later, after performing the same anesthetic protocol, skin and subcutaneous tissues from the implant area and sham incisions were collected and fixed in a container with 10 % formaldehyde solution for posterior histological evaluation. The rats were then euthanized, by lethal intracardiac injection of 5 % sodium pentobarbital (*Euthasil*®).

Afterwards, tissues samples were routinely processed, dehydrated, paraffin embedded, cut and stained with haematoxylin and eosin (H&E). The cross-sections were then examined by a pathologist and semi-quantitatively evaluated according to International Standard (ISO 10993-6) criteria for biological evaluation of the local effects of medical devices after implantation. The objective is to characterize the history and evolution of tissue response after implantation of a medical device/biomaterial including its final integration or degradation. The local effects are evaluated by comparison of the tissue response caused by the tested implant to that caused by the sample or sham controls. The scoring system used for the histological evaluation take into account the extent of the area affected; the presence, number and distribution of polymorphonuclear cells, lymphocytes, plasma cells, macrophages and giant cells; the presence, extent and type of necrosis; other tissue changes such as neovascularization, fatty infiltration, granuloma formation and bone formation and some material parameters such as fragmentation and/or debris presence (Annex B of the ISO 10993-6).

2.2.6 *Antimicrobial profile of the sodium hyaluronate-based hydrogels*

To evaluate the antimicrobial activity of hydrogels *Alg/HA*, *Alg/HA1* and *Alg/HA2,* four different microorganisms and two different techniques were used. The antimicrobial activity of the hydrogel *Alg* was used as null microbial inhibition control.

2.2.6.1 Colony-forming units (CFU) count technique CFU count technique was used for *Staphylococcus aureus*, *Staphylococcus epidermidis* and *Candida albicans* in the presence of the hydrogels *Alg/HA*, *Alg/HA1* and *Alg/HA2*. Firstly, 50 μL of the microbial suspension (1.5×10^4 CFU/mL) were spread onto a plate with solid growth medium (*Liofilchem,* Italy). Then, 2 mL of hydrogel was added and the plates were incubated in aerobic conditions, at 37 °C with 5 % CO_2, for 24 h. After incubation, standard CFU count of each plate was done. This procedure was performed in quadruplicate for each microorganism and for each hydrogel.

2.2.6.2 Inhibitory zone diameters technique This technique was used for *Pseudomonas aeruginosa* bacteria and for this analysis 50 μL of the bacterial suspension (1.5×10^8 CFU/mL) was spread onto the plates with solid medium. Then, sterilized stainless-steel rings with an external diameter of 1 mm (inner diameter, 7 mm) were placed over and filled with 1 mL of sterilized hydrogel. The plates were incubated in aerobic conditions, at 37 °C with 5 % CO_2, for 24 h. After this period, the shortest distance between the outer border of the ring and the first point of bacterial growth was measured. This procedure was performed in triplicate for each hydrogel.

2.2.7 *Statistical analysis*

Experimental data is presented as mean ± SD (standard deviation). Statistical analysis of data was performed using the one-way ANOVA test with Bonferroni post hoc analysis, using the software *SigmaStat* 3.5. The differences were considered to be significant at a level of $p < 0.05$.

3 Results and discussion

3.1 Cell viability evaluation

The viability of MG63 cells seeded on *Alg_IBS*, *Alg/Ch_IBS*, *Alg/HA_IBS* and GR-HA granules was evaluated and compared by the MTT assay where ethanol represents null cell viability. MTT reduction can be generally attributed to mitochondrial succinate dehydrogenase redox activity and as such the results presented in Fig. 1 are proportional to cell metabolism and therefore to cell viability [35].

As observed in Fig. 1, all the tested samples present a cell metabolism increase with time and much higher values than the ethanol control. At 24 h, the association of the

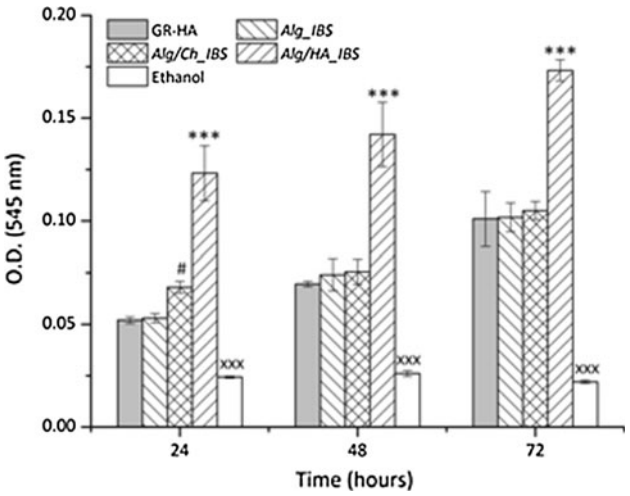

Fig. 1 Viability of MG63 cells seeded on the three developed *IBSs*, after 24, 48 and 72 h of incubation. Data are presented as mean ± SD. $^{***}p < 0.001$: significant difference between *Alg/HA_IBS* and each one of the other samples. $^{xxx}p < 0.001$: significant difference between Ethanol and each one of the other samples. $^{\#}p < 0.05$: significant difference of *Alg/Ch_IBS* compared with *GR-HA* and *Alg_IBS*

hydrogels *Alg/Ch* and *Alg/HA* to GR-HA granules significantly increases the cell viability on the substitute. However, at 48 and 72 h only the association of the hydrogel *Alg/HA* to the GR-HA granules improves the cell viability on the *IBS*. A higher viability can reveal a better cell adaptation to the material, leading to a higher cell production of ECM components and proliferation.

Cell growth and function are influenced by the biomaterial surface characteristics, such as morphology and/or chemical composition. GR-HA is reported as presenting a better osteoblastic growth and function than hydroxyapatite (HAP), due to its triphasic composition: HAP, α- and β-tricalcium phosphate (TCP). These two TCP crystal phases are less stable than HAP, improving the osteoblasts performance due to of ions release to the extra-cellular environment [4, 5]. Moreover, the released ions react with physiologic ions, leading to the formation of a new apatite layer between the implant and bone, promoting the osteointegration [36].

The association of the hydrogels *Alg/Ch* and *Alg/HA* to GR-HA can improve the cell viability due to their morphology and chemical composition. The higher cell metabolism using these two hydrogels, mainly the hydrogel *Alg/HA*, can be explained by the addition of chitosan or hyaluronate to alginate, thus enhancing the bioactive ability of the polymeric vehicle as expected. Chitosan and hyaluronic acid are natural polysaccharides that have the advantage of mimic ECM biological macromolecules, which cells are naturally prepared to recognize and deal with metabolically [13, 14].

3.2 SEM analysis

Cell attachment, adhesion and spreading are very important steps for a good cell/material interaction. The way these phenomena occur influences the cell's ability to proliferate and to differentiate, which is essential for the formation of an implant/bone functional interface and the subsequent biomaterial osteointegration. Therefore, SEM analysis was performed in order to observe cell adhesion to the different injectable systems as well as their morphology.

After 24 h of incubation, it is possible to observe that MG63 cells adhered to the *Alg_IBS, Alg/Ch_IBS* and *Alg/HA_IBS* surfaces, even though the cells present different morphologies, as observed in Fig. 2a2–c2. The cells seeded on the *Alg_IBS* surface have a spherical shape with some visible lamellipodia. Two different cell adhesion stages can be distinguished on the *Alg/Ch_IBS* surface, cells with a spherical morphology and lamellipodia can be observed, which indicate an initial stage of adhesion, and a more advanced stage where the osteoblast-like cells have a spread morphology and some filopodia. On the *Alg/HA_IBS* surface, after just 1 day of incubation, cells have a spreader shape with more developed filopodia.

The distinct cell morphology on the three *IBS*s can be explained by the different cells/material interaction, which is influenced by the implant surface properties [5, 37]. What mainly distinguishes the *IBS*s surfaces is the polymeric vehicle that is associated with the GR-HA. Thus, the objective of improving the cell adhesion phenomenon on the bone substitute by associating a bioactive polymer to an alginate vehicle was successfully achieved, as expected according to the literature [21, 38].

Chitosan structure resembles the glycosaminoglycans of the bone extracellular matrix, and it has been reported that it can act as a promoter of cell adhesion, mainly due to its positively charged surface which will attract the negatively charged cell surface [21, 22]. Hyaluronic acid is the main component of the living tissues extracellular matrix (ECM), namely in the connective tissue, being involved in cell signaling and matrix organization [23–25]. Its incorporation in the *IBS* allows it to mimic the organic part of the bone ECM, while GR-HA mimics the inorganic part of the tissue. This synergy can lead to a better cell adhesion and spreading. This polymer is able to interact with different cell surface receptors, establishing several sites of adhesion between cells and the material surface [39]. In a cell adhesion process, during the establishment of the adhesion sites between cells and the material surface, there is a specific degree of organization and production of the cell cytoskeleton filamentous proteins, namely of the actin filaments. They tend to assemble in long bundles leading to protrusions (filopodia)

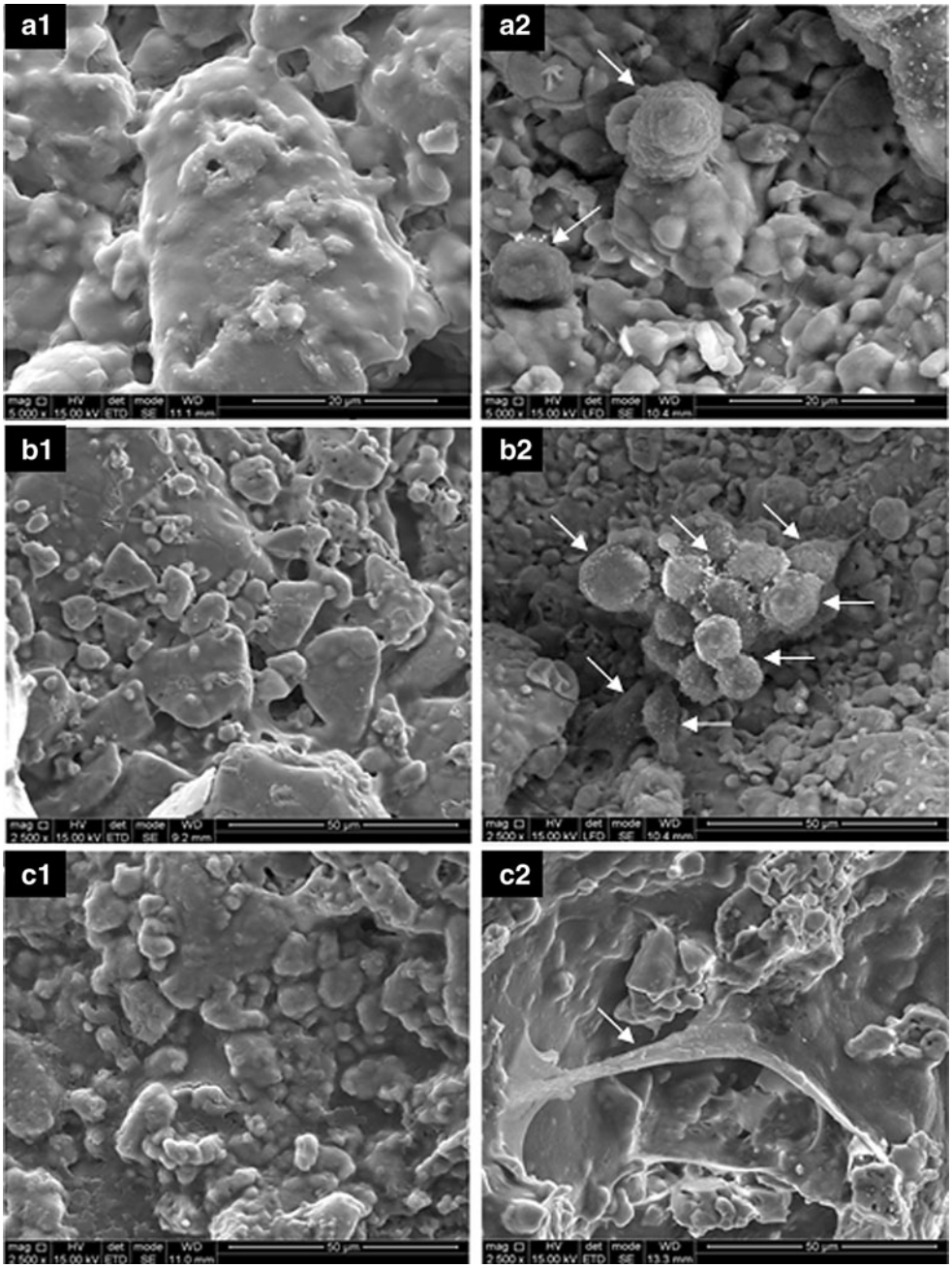

Fig. 2 SEM appearance of the MG63 cells adhered on the three developed IBSs after 24 h of incubation: A1-*Alg_IBS* non-cell seeded; A2-*Alg_IBS* cell seeded; B1-*Alg/Ch_IBS* non-cell seeded; B2-*Alg/Ch_IBS* cell seeded; C1-*Alg/HA_IBS* non-cell-seeded; C2-*Alg/HA_IBS* cell seeded. The *arrows* indicate cells adhered on the materials

of the plasma membrane, so the cells can stretch out on the material surface, thus presenting a spreader shape [37, 40–42].

The cytoskeleton organization controls the cell morphology, and once its proteins are involved in signal transduction the cell shape can also be related with cell growth and function [42, 43]. In fact, when cells try to adhere to the surface of a material, mitochondrial activity increases due to the energy production necessary to synthesize the above-mentioned proteins that are crucial to cell adhesion. Since MTT measure mitochondrial activity and by extension cell viability, the process of cell adhesion is close-related to cell viability [44]. In this work the *Alg/HA_IBS* presented cells with the spreader and organized structure and so it also presented the highest viability, as discussed previously.

3.3 Subcutaneous implantation

After in vitro characterization, the *Alg/AH* hydrogel that showed the best performance was evaluated by subcutaneous implantation in Sprague–Dawley® rats, to assess the tissue local biological response to this hydrogel. Throughout 2 weeks follow-up time, all animals remained healthy and none developed local or systemic signs of infection and/or inflammation were observed. Using a descriptive analysis and a scoring system according to Standard ISO 10993-6, the following criteria were considered for semi-quantitative histological study of the tissue around the implanted material: collagen fibers formation, inflammatory infiltrate, the presence of necrosis and other tissue alterations such as vascularization, lipid infiltration.

To determine the biological response of the biomaterial, the result of the control subcutaneous tissue (*SC tissue* (T_0)) was first determined (5.0), as presented in Table 1. Then, according to the same evaluation method, the sham samples (*Sham* 1 and *Sham* 2) were analyzed and the average of the samples was estimated (27.57). In turn, the mean of these two variables represents the value of the control to be considered, in order to remove the inflammation grade that rats usually present in their subcutaneous tissue and to underestimate the effects of the surgical and suture techniques (16.29). The tissue area around the hydrogel *Alg/HA* (*SC tissue (Alg/HA)*) was also evaluated and the ISO score determined (23.22). Finally, the sample biological response, i.e. the inflammation caused only by the biomaterial, was achieved by subtracting the value of the control to the value of the *SC tissue (Alg/HA)* (6.93). By ISO 10993-6, this result corresponds to a slight irritating response, thus making this material biocompatible and adequate for in vivo application.

Table 1 Results of the biological response to the implanted material, according to ISO 10993-6

Cell type/response	SC Tissue (T_u) Average	Sham 1	Sham 2	SC Tissue (Alg/HA)
Neutrophilis	0.00	0.71	1.85	0.33
Lymphocytes	1.00	3.00	3.00	2.89
Plasma cells	0.33	2.85	3.00	2.33
Macrophages	0.57	3.00	2.85	3.89
Giant cells	0.00	1.71	0.57	0.11
Necrosis	0.00	0.43	0.00	0.00
Sub-total (×2)	4.00	23.43	22.57	19.11
Neovascularization	1.00	2.57	3.00	2.78
Fibrosis	0.00	1.43	2.14	1.33
Lipid infiltration	0.00	0.00	0.00	0.00
Sub-total	1.00	4.00	5.14	4.11
Total	5.0	27.43	27.71	23.32

Sham average = (27.43 + 27.21)/2 = 27.57. Control average = (27.57 + 5.0)/2 = 16.29. Biological response of *Alg/HA* hydrogel = 23.22 − 15.29 = 6.93

The distinction between the various inflammatory cells was performed in accordance with the classical morphological characteristics of each cell population where various lymphocytes and plasma cells are visible in Fig. 3. Such histological findings are in agreement with an attempt at healing by connective tissue replacement of damaged tissue, strengthened by the presence of macrophages since these cells play a critical role in the initiation, maintenance and resolution of inflammation. Quantitatively, Table 1 indicates the very low number of neutrophils and giant cells (not seen in Fig. 3), and even the absence of necrosis and lipid infiltration. Neovascularization and fibrosis are clearly visible in Fig. 3, typical of tissue regeneration process.

3.4 Antimicrobial profile of the sodium hyaluronate-based hydrogels

Every surgical procedure, even a less invasive one, presents susceptibility to infections, which can compromise the success of the implanted material. Several approaches are used to prevent those infections, namely the use of sterility protocols and the antibiotics administration. However, those protocols are not always effective and the use of antibiotics can induce bacterial resistance that inhibits their effect [29, 30]. Thus, the use of a vehicle with the ability to decrease or inhibit the growth of several microorganisms could significantly improve the clinical outcomes of the bone substitute usage [29, 45]. In order to achieve that purpose, it was decided to incorporate in the hydrogel ions with antimicrobial properties. Silver (Ag), for instance, has already been reported as an effective antibacterial agent, but it has also been reported as a cytotoxic agent [46]. Ce(III) ions have also been reported as having a bacteriostatic and bactericidal effect [31, 33].

Therefore, the hydrogel, that revealed the better biological performance in vitro and a good response in vivo, was modified in an attempt to obtain a bioactive vehicle also with potential antimicrobial properties. Thus, Ce(III) ions were incorporated in hydrogel *Alg/HA* in two different concentrations: *Alg/HA1* and *Alg/HA2*.

In order to perform a deeper analysis, the sodium hyaluronate-based hydrogels antimicrobial properties were evaluated against the main bacteria responsible for infections in hospital environment, namely in orthopedic surgical procedures, and even against the most prevalent fungus [29, 45, 47, 48]. In order to determine the growth of such microbes in the presence of each tested hydrogel, two different techniques were used. *S. aureus*, *S. epidermidis*

and *C. albicans* grow to form individual colonies, which are countable. *P. aeruginosa* forms irregular spots, which sometimes are overlapping, thus making the inhibitory zone diameters technique more appropriate to use.

As presented in Fig. 4, the hydrogel *Alg/HA* shows antimicrobial activity against all tested microorganisms when compared with the hydrogel *Alg* (considered as null antimicrobial activity control). These results indicate that hyaluronic acid has an antimicrobial effect, which is in accordance with the literature including the lower effect against *P. aeruginosa* [45].

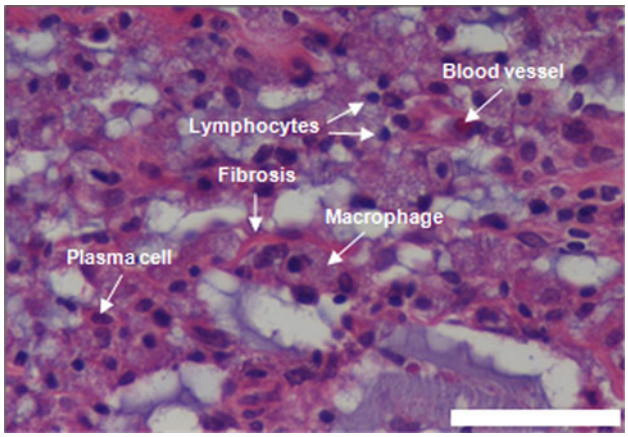

Fig. 3 Histological image of skin and subcutaneous tissues from the implant area (SC tissue (*Alg/HA*)), after 2 weeks of the hydrogel *Alg/HA* implantation; *scale bar*: 100 μm

Hyaluronic acid has previously shown to have a wide bacteriostatic effect, namely against microbes commonly found in orthopaedic practice and oral cavity [45]. This polymer can induce the expression of some innate immunity antibiotic peptides, such as β-defensin 2 produced by epithelial cells, which exhibits antimicrobial activity [49, 50]. However, in this work it was tried to improve the antimicrobial ability of the hydrogel even more, promoted by the hyaluronic acid, by incorporating Ce(III) ions.

Regarding the Ce(III) antimicrobial ability, it is observed in Fig. 4 that the addition of this ion enhanced the antimicrobial activity of the hydrogel *Alg/HA*. For *S. aureus*, *S. epidermidis* and *C. albicans*, hydrogel *Alg/HA1* presents a significant antimicrobial activity increase compared to the hydrogel *Alg/HA*. A higher Ce(III) concentration in the hydrogel *Alg/HA2*, for these microorganisms, leads to an even stronger activity. Concerning *P. aeruginosa*, it is necessary to add to the hydrogel *Alg/HA* the highest tested Ce(III) concentration to verify a significant antibacterial effect increase. This bacterium higher resistance to the ion, when comparing to others microorganisms, has already been verified [32].

Cerium is reported as having bacteriostatic and bactericidal activity against several bacteria and also antimicrobial effect against fungi [51]. Regarding its way of action, some possible mechanisms have been postulated: the uptake of cerium into the cytoplasm can inhibit the cellular respiration, oxygen uptake and glucose metabolism, or eventually the disruption of cell membrane [31, 32]. *P. aeruginosa*, being a gram-negative bacterium, has a more complex cell

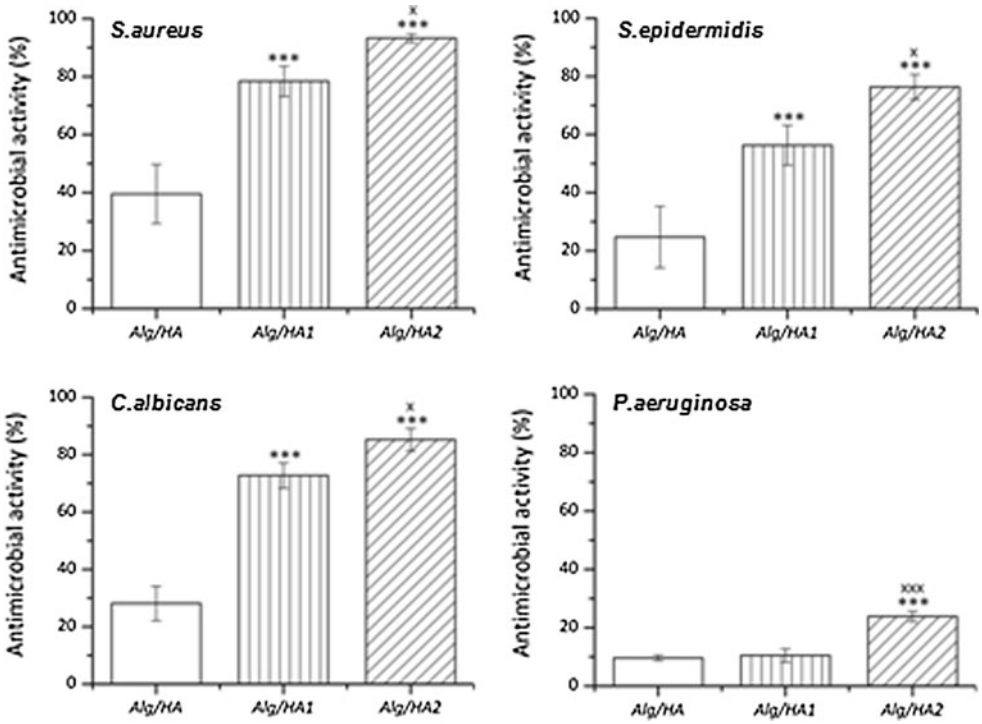

Fig. 4 Antimicrobial activity of the hydrogels *Alg/HA*, *Alg/HA1* and *Alg/HA2* after 24 h of incubation. Values were obtained using the hydrogel *Alg* as model of null inhibition. Data are presented as mean ± SD. ***$p < 0.001$: significant difference compared with *Alg/HA*

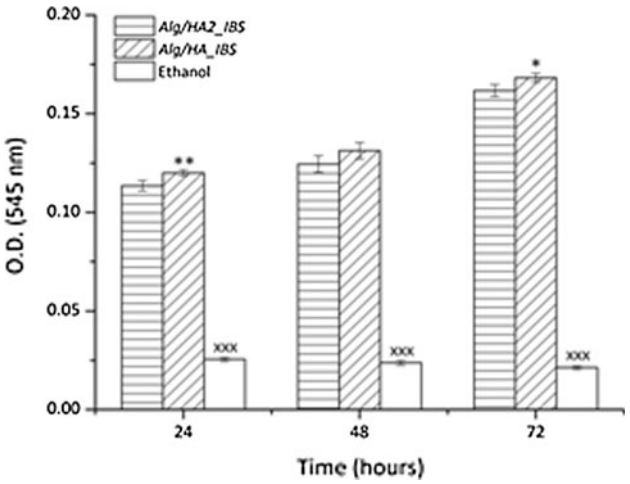

Fig. 5 Viability of MG63 cells seeded on *Alg/HA2_IBS* and *Alg/HA_IBS*, after 24, 48 and 72 h of incubation. Data are presented as mean ± SD. $*p < 0.05$, $**p < 0.002$: significant difference compared with *Alg/HA2_IBS*. $^{xxx}p < 0.001$: significant difference between Ethanol and each one of the other samples

wall than the gram-positive bacteria (*S. aureus* and *S. epidermidis*). Its cell wall is composed by a peptidoglycan layer and a lipidic external membrane, being less permeable and susceptible to biocides than the gram-positive bacteria. Thus, the weaker effect of Ce(III) in this microbe can be explained by the difficulty of Ce(III) to enter and interfere in cellular events.

3.5 Cell viability evaluation on the *Alg/HA2_IBS*

The MTT assay was performed in order to evaluate if Ce(III) incorporation in the hydrogel *Alg/HA* influences the MG63 cells metabolism in contact with the *IBS*. Thus, the cell viability on *Alg/HA_IBS* was compared with the one on *Alg/HA2_IBS*, since the hydrogel *Alg/HA2* presented the highest antimicrobial activity for all tested microorganisms.

It is clear, in Fig. 5, that the cell viability promoted by the *Alg/HA_IBS* and *Alg/HA2_IBS* increases over time. Nevertheless, the *Alg/HA2_IBS* presents a slightly lower viability than the *Alg/HA_IBS* at 24 and 72 h. Despite this reduction, about 5.42 ± 0.28 % at 24 h and 5.14 ± 0.25 % at 72 h, cell metabolism on *Alg/HA2_IBS* is still much higher than the one verified on GR-HA granules alone. Therefore, by using Ce(III) ions it is possible to obtain a hydrogel with an effective antimicrobial ability without interfering with cells viability improvement, as desired.

It has been reported that lanthanides do not penetrate mammalian cell membranes as it happens with bacteria [32, 52]. Nevertheless, Ce(III) radius is very similar to the Ca^{2+} one, therefore, Ce(III) is able to interact with calcium-dependent transmembrane signaling channels, by which can interfere with intracellular events and cause a decrease in the viability of osteoblasts [32, 52]. However, this Ce(III) competition with Ca^{2+} can also have advantages, namely inhibitory effect on mast cells degranulation and histamine release from both these cells and basophils, by interference with a cell membrane ATPase pump [32, 52].

4 Conclusions

Firstly, it was verified that the hydrogel association to the GR-HA granules can enhance the osteoblasts viability of the bone substitute, mainly by the hydrogel *Alg/HA*. Besides, the cell adhesion and morphology on the *IBS*s was influenced by the polymeric composition of the associated hydrogel. In vivo experiments showed that the hydrogel *Alg/HA* caused a slightly irritating response indicating its biocompatibility, thus making it useful in biomedical applications.

The association of hyaluronic acid with alginate increased the antimicrobial effect against the tested microorganisms. Moreover, Ce(III) addition to the hydrogel *Alg/HA* enhances its antimicrobial activity without compromise the hydrogel cell viability.

Overall, these results show that the hydrogel *Alg/HA2* is a very promising vehicle to associate with a synthetic bone substitute. This hydrogel, besides allowing the granules injection, also enhances the osteoconductive ability of the substitute and even grant it an antimicrobial activity improving its regenerative performance.

Acknowledgments The authors would like to acknowledge the financial support from FCT (Fundação para a Ciência e a Tecnologia) through the grant SFRH/BD/76237/2011 and project ENMED/0002/2010, from FEDER funds through the program COMPETE—Programa Operacional Factores de Competitividade—under the project PEst-C/EME/UI0285/2011, as well as to the project I&DT BIOMAT&CELL n. 1372.

References

1. Giannoudis PV, Dinopoulos H, Tsiridis E. Bone substitutes: an update. Injury. 2005;36:20–7.
2. Bostrom MPG, Seigerman DA. The clinical use of allografts, demineralized bone matrices, synthetic bone graft substitutes and osteoinductive growth factors: a survey study. HSS J. 2005; 1:9–18.
3. Lopes MA, Knowles JC, Santos JD. Structural insights of glass-reinforced hydroxyapatite composites by rietveld refinement. Biomaterials. 2000;21:1905–10.
4. Gutierres M, Lopes MA, Sooraj Hussain N, Lemos AF, Ferreira JMF, Afonso A, et al. Bone ingrowth in macroporous Bonelike® for orthopaedic applications. Acta Biomat. 2008;4:370–7.
5. Lopes MA, Knowles JC, Santos JD, Monteiro FJ, Olsen I. Direct and indirect effects of P_2O_5 glass reinforced-hydroxyapatite composites on the growth and function of osteoblast-like cells. Biomaterials. 2000;21:1165–72.

6. Liu H, Li H, Cheng W, Yang Y, Zhu M, Zhou C. Novel injectable calcium phosphate/chitosan composites for bone substitute materials. Acta Biomat. 2006;2(5):557–65.
7. Larsson S, Hannink G. Injectable bone-graft substitutes: current products, their characteristics and indications, and new developments. Injury. 2011;42:30–4.
8. Martínez-Sanz E, Ossipov DA, Hilborn J, Larsson S, Jonsson KB, Varghese OP. Bone reservoir: injectable hyaluronic acid hydrogel for minimal invasive bone augmentation. J Control Release. 2011;152:232–40.
9. Gaharwar AK, Dammu SA, Canter JM, Wu C, Schmidt G. Highly extensible, tough, and elastomeric nanocomposite hydrogels from poly(ethylene glycol) and hydroxyapatite nanoparticles. Biomacromolecules. 2011;12:1641–50.
10. Oliveira SM, Almeida IF, Costa PC, Barrias CC, Ferreira MRP, Bahia MF, et al. Characterization of polymeric solutions as injectable vehicles for hydroxyapatite microspheres. AAPS PharmSciTech. 2010;11:852–8.
11. Couto D, Hong Z, Mano J. Development of bioactive and biodegradable chitosan-based injectable systems containing bioactive glass nanoparticles. Acta Biomat. 2009;5:115–23.
12. Vaccaro AR. The role of the osteoconductive scaffold in synthetic bone graft. Orthopedics. 2002;25:571–8.
13. Mano JF, Silva GA, Azevedo HS, Malafaya PB, Sousa RA, Silva SS, et al. Natural origin biodegradable systems in tissue engineering and regenerative medicine: present status and some moving trends. J R Soc Interface. 2007;4:999–1030.
14. Slaughter BV, Khurshid SS, Fisher OZ, Khademhosseini A, Peppas NA. Hydrogels in regenerative medicine. Adv Mater. 2009;21:3307–29.
15. Wang L, Shelton RM, Cooper PR, Lawson M, Triffitt JT, Barralet JE. Evaluation of sodium alginate for bone marrow cell tissue engineering. Biomaterials. 2003;24:3475–81.
16. West E, Xu M, Woodruff T, Shea L. Physical properties of alginate hydrogels and their effects on in vitro follicle development. Biomaterials. 2007;28:4439–48.
17. Sriamornsak P, Thirawong N, Korkerd K. Swelling, erosion and release behavior of alginate-based matrix tablets. Eur J Pharm Biopharm. 2007;66:435–50.
18. Ulery BD, Nair LS, Laurencin CT. Biomedical applications of biodegradable polymers. J Polym Sci B. 2011;49:832–64.
19. Andersen T, Strand BL, Formo K, Alsberg E, Christensen BE. Alginates as biomaterials in tissue engineering. J Carbohydr Chem. 2012;37:227–58.
20. Nair LS, Laurencin CT. Biodegradable polymers as biomaterials. Prog Polym Sci. 2007;32:762–98.
21. Chen A, Haddad D, Wang R. Analysis of chitosan-alginate bone scaffolds. Newark: New Jersey Governor's School of Engineering & Technology; 2009. p. 1–8.
22. Aranaz I, Mengíbar M, Harris R, Paños I, Miralles B, Acosta N, et al. Functional characterization of chitin and chitosan. Curr Chem Biol. 2009;3:203–30.
23. Brown MB, Jones SA. Hyaluronic acid: a unique topical vehicle for the localized delivery of drugs to the skin. J Eur Acad Dermatol. 2005;19:308–18.
24. Prestwich GD. Hyaluronic acid-based clinical biomaterials derived for cell and molecule delivery in regenerative medicine. J Control Release. 2011;155:193–9.
25. Kim J, Kim IS, Cho TH, Lee KB, Hwang SJ, Tae G, et al. Bone regeneration using hyaluronic acid-based hydrogel with bone morphogenic protein-2 and human mesenchymal stem cells. Biomaterials. 2007;28:1830–7.
26. Patterson J, Siew R, Herring SW, Lin ASP, Guldberg R, Stayton PS. Hyaluronic acid hydrogels with controlled degradation properties for oriented bone regeneration. Biomaterials. 2010;31:6772–81.
27. Martínez-Sanz E, Ossipov DA, Hilborn J, Larsson S, Jonsson KB, Varghese OP. Bone reservoir: injectable hyaluronic acid hydrogel for minimal invasive bone augmentation. J Control Release. 2011;152:232–40.
28. Nagaoka I, Igarashi M, Sakamoto K. Biological activities of glucosamine and its related substances. Adv Food Nutr Res. 2012;65:337–52.
29. Campoccia D, Montanaro L, Arciola CR. The significance of infection related to orthopedic devices and issues of antibiotic resistance. Biomaterials. 2006;27:2331–9.
30. Campoccia D, Montanaro L, Speziale P, Arciola CR. Antibiotic-loaded biomaterials and the risks for the spread of antibiotic resistance following their prophylactic and therapeutic clinical use. Biomaterials. 2010;31:6363–77.
31. Cobrado L, Azevedo MM, Silva-Dias A, Ramos JP, Pina-Vaz C, Rodrigues AG. Cerium, chitosan and hamamelitannin as novel biofilm inhibitors? J Antimicrob Chemoth. 2012;67:1159–62.
32. Garner JP, Heppell PSJ. Cerium nitrate in the management of burns. Burns. 2005;31:539–47.
33. Zhang H, Feng J, Zhu W, Liu C, Gu J. Bacteriostatic effects of cerium–humic acid complex. Biol Trace Elem Res. 1999;73:29–36.
34. Morais DS, Rodrigues MA, Silva TI, Lopes MA, Santos M, Santos JD, Botelho CM. Development and characterization of novel alginate-based hydrogels as vehicles for bone substitutes. Carbohydr Polym. 2013;95(1):134–42.
35. Takahashi S, Abe T, Gotoh J, Fukuuchi Y. Substrate-dependence of reduction of MTT: a tetrazolium dye differs in cultured astroglia and neurons. Neurochem Int. 2002;40(5):441–8.
36. Dee KC, Puleo DA, Bizios R, editors. An introduction to tissue-biomaterial interactions. New York: Wiley; 2002.
37. Hempel U, Hefti T, Dieter P, Schlottig F. Response of human bone marrow stromal cells, MG-63, and SaOS-2 to titanium-based dental implant surfaces with different topography and surface energy. Clin Oral Implants Res. 2011;24(2):1–9.
38. Chunga TW, Yangb J, Akaikeb T, Choc KY, Nahd JW, Kima SI, et al. Preparation of alginate/galactosylated chitosan scaffold. Biomaterials. 2001;23:2827–34.
39. Zaleski KJ, Kolodka T, Cywes-Bentley C, McLoughlin RM, Delaney ML, Charlton BT, et al. Hyaluronic acid binding peptides prevent experimental staphylococcal wound infection. Antimicrob Agents Chemother. 2006;50:3856–60.
40. Anselme K. Osteoblast adhesion on biomaterials. Biomaterials. 2000;21(7):667–81.
41. Wutticharoenmongkol P, Pavasant P, Supaphol P. Osteoblastic phenotype expression of MC3T3-E1 cultured on electrospun polycaprolactone fiber mats filled with hydroxyapatite nanoparticles. Biomacromolecules. 2007;8:2602–10.
42. Gwynn IA. Cell biology at interfaces. J Mater Sci Mater Med. 1994;5:357–60.
43. Amaral M, Costa MA, Lopes MA, Silva RF, Santos JD, Fernandes MH. Si_3N_4-bioglass composites stimulate the proliferation of MG63 osteoblast-like cells and support the osteogenic differentiation of human bone marrow cells. Biomaterials. 2002;23(24):4897–906.
44. Yang D, Lü X, Hong Y, Xi T, Zhang D. The molecular mechanism of mediation of adsorbed serum proteins to endothelial cells adhesion and growth on biomaterials. Biomaterials. 2013;34:5747–58.
45. Carlson GA, Dragoo JL, Samimi B, Bruckner DA, Bernard GW, Hedrick M, et al. Bacteriostatic properties of biomatrices against common orthopaedic pathogens. Biochem Biophys Res Commun. 2004;321:472–8.
46. Lima R, Seabra AB, Durán N. Silver nanoparticles: a brief review of cytotoxicity and genotoxicity of chemically and biogenically synthesized nanoparticles. J Appl Toxicol. 2012;32:867–79.

47. Peleg AY, Hooper DC. Hospital-acquired infections due to gram-negative bacteria reply. New Engl J Med. 2010;363: 1483–4.
48. Diba K, Rhaimirad M, Makhdoomi K, Khorshidvand Z. Identification of Candida species isolated from hospital acquired infections cases and hospital indoor environments. Afr J Microbiol Res. 2012;6:4164–8.
49. Palffy R, Gardlik R, Behuliak M, Kadasi L, Turna J, Celec P. On the physiology and pathophysiology of antimicrobial peptides. Mol Med. 2009;15:51–9.
50. Gariboldi S, Palazzo M, Zanobbio L, Selleri S, Sommariva M, Sfondrini L, et al. Low molecular weight hyaluronic acid increases the self-defense of skin epithelium by induction of beta-defensin 2 via TLR2 and TLR4. J Immunol. 2008;181:2103–10.
51. Amara SG, Gudermann T, Jahn R, Lill R, Nilius B, Offermanns S, et al., editors. Reviews of physiology, biochemistry and pharmacology. Netherlands: Springer; 2005.
52. Jakupec MA, Unfried P, Keppler BK. Pharmacological properties of cerium compounds. Rev Physiol Biochem Pharmacol. 2005; 153:101–11.